

Applications of Strain Gradient Theories to the Size Effect in Submicro-Structures incl. Experimental Analysis of Elastic Material Parameters

Christian Liebold^{a*} and Wolfgang H. Müller^a

^a*Berlin University of Technology, Institute of Mechanics,
Einsteinufer 5, 10587 Berlin, Germany*

(Received February 25, 2015; Revised June 27, 2015; Accepted July 1, 2015)

Strain gradient theories of elasticity are used for the description of the so-called size effect: Materials in (sub-) micro-structures show a stiffer elastic response, *e.g.*, during bending. A quantitative understanding of the size effect is important during the design phase of micro- and nanosized systems which, for example, may be accompanied by Finite Element (FE) simulations. Special attention will be paid to a specific higher-order theory known as the so-called modified strain gradient theory of linear elasticity, which goes beyond the limits of the classical Boltzmann continuum. The objectives of this paper are to determine the material length scale parameters by analyzing experimental data obtained from force-displacement measurements using extremely small cantilever beams. The corresponding data is studied with analytical as well as numerical tools based on higher gradient theory. In particular, deflection measurements were performed and force data was recorded for submicron beams made of epoxy and SU-8. Bending rigidities were measured with the help of atomic force microscopy. An analytical solution of Euler-Bernoulli beam theory is presented incorporating the necessities of the extended theory. In contrast to existing work on the formulation of the strain gradient theory in terms of an FE-formulation and analysis, the crucial differential equation developed here is consistently based on the balance of linear momentum and on the balance of moment of momentum. The obtained data from the finite element modeling, the derived analytical formulae and the obtained data from the experiments is used for the evaluation of higher gradient coefficients.

Keywords: Strain gradient theory, Couple stress theory of elasticity, Finite elements, Variational formulation.

AMS Subject Classification: 53Z06, 74Q06, 74M25, 74K10, 74A30, 74A35.

1. Introduction

A quantitative understanding of the so-called size effect in micro- and submicrostructures is of great importance during modeling of Micro- and Nanoelectromechanical Systems (MEMS/NEMS). A size effect on the micro- and on the nanoscale is, for example, reflected in a stiffer elastic response to external loads. This has been observed in metals and polymers deforming plastically [7, 8]. As far as a size effect in elasticity is concerned, LAM *et al.* (2003) [10] observed an increase in bending rigidities of micro-beams made of epoxy. The values for the bending rigidities were about 2.4 times larger than predicted by conventional theory, when the beam thicknesses decreased from 120 to 20 μm . MCFARLAND *et al.* (2005) [13] have observed

*Corresponding author. Email: christian.liebold@tu-berlin.de

similar variations in the bending rigidities of polypropylene micro cantilevers, also within the linear elastic regime. Analogously, other experiments have shown an apparent increase in YOUNG's modulus without referring to higher-order theories [3, 11]. LAM *et al.* (2003) [10] have shown that in the absence of strain gradients (for example, in uniaxial tensile tests) the elastic behavior of epoxy is independent of the thickness of the sample, which is confirmed by strain gradient models.

Conventional theories based on the BOLTZMANN (a.k.a. CAUCHY) continuum are not able to predict a size effect. In the present work the *strain gradient theory* is used as a so-called continuum theory of higher-order. First works on the development of couple stress theories by, *e.g.*, TOUPIN (1962) [16], MINDLIN & TIERSTEN (1962) [14], KOITER (1964) [9] and MINDLIN & ESHEL (1968) [15] contain second order derivatives of the displacement vector to account for quantities such as curvature or rotation. It was not before the introduction of second order derivatives in terms of higher-order constitutive relations and energy considerations, that a generalization of a strain gradient continuum had been achieved and ERINGEN proposed "nonsimple materials of the gradient type" [5] in order to derive the corresponding higher-order material dependencies.

2. Modified strain gradient theories

The starting point of the present study is the evaluation of one of the three reduced forms of the higher-order strain energy densities for small deformations u^{SG} ("SG" = Strain Gradient), postulated by MINDLIN (1962) [14]. In the following, we make use of the EINSTEIN summation convention on repeated indices. Spatial partial derivatives in a Cartesian coordinate system are denoted by comma-separated indices. MINDLIN's various representations of the strain energy density read:

$$u^{\text{SG}} = u^{\text{1ST}}(\varepsilon_{ij}, \eta_{ijk}) = u^{\text{2ND}}(\varepsilon_{ij}, \tilde{\eta}_{ijk}) = u^{\text{3RD}}(\varepsilon_{ij}, \bar{\eta}_{ij}, \bar{\bar{\eta}}_{ijk}) , \quad (1)$$

where $\varepsilon_{ij} = u_{(i,j)} = \frac{1}{2}(u_{i,j} + u_{j,i})$ denotes the small strain tensor (or the symmetric part of the gradient of displacement), $\eta_{ijk} = u_{k,ij}$ the second gradient of displacement, $\bar{\bar{\eta}}_{ijk} = \frac{1}{3}(u_{k,ij} + u_{i,jk} + u_{j,ki})$ the symmetric part of the second gradient of displacement, $\tilde{\eta}_{ijk} = \frac{1}{2}(u_{k,ij} + u_{j,ki}) = \varepsilon_{kj,i}$ the gradient of strain, $\bar{\eta}_{ij} = \varphi_{i,j} = \frac{1}{2}\epsilon_{ilk} u_{k,lj}$ the gradient of rotation, $\varphi_i = \frac{1}{2}\epsilon_{ijk} u_{k,j}$ the macroscopic rotation vector, and ϵ_{ijk} the alternating tensor (or LEVI-CIVITA symbol). The corresponding work-conjugated stress measures of the first form are [4]:

$$\sigma_{ij} = \frac{\partial u^{\text{1ST}}}{\partial \varepsilon_{ij}} \quad \text{and} \quad \mu_{ijk} = \frac{\partial u^{\text{1ST}}}{\partial \eta_{ijk}} , \quad (2)$$

if linear elastic material behavior is assumed. σ_{ij} and μ_{ijk} denote the CAUCHY stress tensor and the hyper- (or double-) stress tensor, respectively. For nonsimple materials of the gradient type a linear-elastic strain energy density of the first form results in:

$$u^{\text{1ST}} = C_{ijkl} \varepsilon_{kl} \varepsilon_{ij} + D_{ijklmn} \eta_{lmn} \eta_{ijk} + B_{ijklo} \eta_{klo} \varepsilon_{ij} , \quad (3)$$

where C_{ijkl} and D_{ijklmn} are the elastic and higher order elastic constants and B_{ijklo} denote coupling constants [2]. These will vanish for the material symmetry class of isotropic materials and then the linear-elastic strain energy density reduces to [4, 15]:

$$2u^{1ST} = \alpha_1 \varepsilon_{ij} \varepsilon_{ij} + \alpha_2 \varepsilon_{kk} \varepsilon_{mm} + \beta_1 \eta_{ijk} \eta_{ijk} + \beta_2 \eta_{iik} \eta_{ljk} \\ + \beta_3 \eta_{iik} \eta_{kjj} + \beta_4 \eta_{ijj} \eta_{ikk} + \beta_5 \eta_{ijk} \eta_{kji} , \quad (4)$$

where α_1 and α_2 are identified as LAMÉ's constants, whereas $\beta_{1,\dots,5}$ represent five additional material parameters. In order to reduce the number of independent additional material parameters from five to three, a decomposition of the second gradient of displacement η_{ijk} (as introduced by FLECK & HUTCHINSON (1997) [6]) is used in combination with making use of the macroscopic rotation vector φ_i . The symmetric part of the second order deformation gradient $\bar{\eta}_{ijk}$ (see Fig. 1) reads:

$$\bar{\eta}_{ijk} = \frac{1}{3} (u_{k,ij} + u_{i,jk} + u_{j,ki}) . \quad (5)$$

$\bar{\eta}_{ijk}$ is further decomposed into a spherical part $\eta_{ijk}^{(0)}$ and into a deviatoric part $\eta_{ijk}^{(1)}$:

$$\eta_{ijk}^{(0)} = \frac{1}{5} (\delta_{ij} \bar{\eta}_{mmk} + \delta_{jk} \bar{\eta}_{mmi} + \delta_{ki} \bar{\eta}_{mmj}) \quad \text{and} \quad \eta_{ijk}^{(1)} = \bar{\eta}_{ijk} - \eta_{ijk}^{(0)} . \quad (6)$$

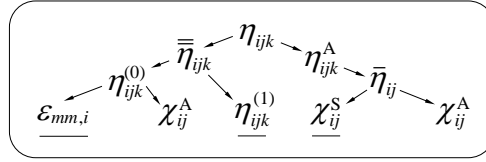


Figure 1. Scheme of decomposition of the second order gradient of displacement.

With the help of the definition of the macroscopic rotation vector φ_i and the anti-symmetric part of its gradient $\chi_{ij}^A = \frac{1}{2} (\varphi_{i,j} - \varphi_{j,i})$, two relations can be obtained: First, the spherical part of the second order deformation gradient $\eta_{ijk}^{(0)}$ can be decomposed into $\varepsilon_{mm,i}$ and χ_{ij}^A ; second, it can be shown that the anti-symmetric part of η_{ijk} will completely depend on the gradient of rotation $\bar{\eta}_{ij}$, *i.e.*:

$$(i): \quad \bar{\eta}_{mmi} = \varepsilon_{mm,i} + \frac{2}{3} \varepsilon_{iln} \chi_{ln}^A , \quad (7)$$

and

$$(ii): \quad \eta_{ijk}^A = \frac{2}{3} (\varepsilon_{ikl} \bar{\eta}_{lj} + \varepsilon_{jkl} \bar{\eta}_{li}) . \quad (8)$$

When assuming symmetry for the couple stress tensor μ_{ij} (the work-conjugate of the gradient of rotation), as proposed by [19], the anti-symmetric part of the gradient of rotation does not affect the strain energy. In summary, the linear-elastic strain energy density for isotropic nonsimple materials of the gradient type u^{MSG} reads in

its modified form (“MSG” = Modified Strain Gradient):

$$\begin{aligned}
u^{\text{MSG}} &= \hat{u} \left(\varepsilon_{ij}, \varepsilon_{mm,i}, \eta_{ijk}^{(1)}, \chi_{ij}^{\text{S}} \right) \\
&= \frac{1}{2} \sigma_{ij} \varepsilon_{ij} + \frac{1}{2} p_i \varepsilon_{mm,i} + \frac{1}{2} \mu_{ijk}^{(1)} \eta_{ijk}^{(1)} + \frac{1}{2} \mu_{ij} \chi_{ij}^{\text{S}} \\
&= \frac{1}{2} \lambda \varepsilon_{ii} \varepsilon_{kk} + \mu \varepsilon_{ij} \varepsilon_{ij} + \mu \ell_0^2 \varepsilon_{mm,i} \varepsilon_{mm,i} + \mu \ell_1^2 \eta_{ijk}^{(1)} \eta_{ijk}^{(1)} + \mu \ell_2^2 \chi_{ij}^{\text{S}} \chi_{ij}^{\text{S}},
\end{aligned} \tag{9}$$

where the corresponding work-conjugated stress measures are:

$$\begin{aligned}
\sigma_{ij} &= \frac{\partial u^{\text{MSG}}}{\partial \varepsilon_{ij}} = \lambda \varepsilon_{kk} \delta_{ij} + 2\mu \varepsilon_{ij}, & p_i &= \frac{\partial u^{\text{MSG}}}{\partial \varepsilon_{mm,i}} = 2\mu \ell_0^2 \varepsilon_{mm,i} \\
\mu_{ijk}^{(1)} &= \frac{\partial u^{\text{MSG}}}{\partial \eta_{ijk}^{(1)}} = 2\mu \ell_1^2 \eta_{ijk}^{(1)}, & \mu_{ij} &= \frac{\partial u^{\text{MSG}}}{\partial \chi_{ij}^{\text{S}}} = 2\mu \ell_2^2 \chi_{ij}^{\text{S}},
\end{aligned} \tag{10}$$

involving the CAUCHY force stress tensor, σ_{ij} , the couple stress tensor, μ_{ij} , and two further higher-order material stress measures, p_i and $\mu_{ijk}^{(1)}$.

3. A finite Element approach to a reduced MSG model

Various papers on the Finite Element Method (FEM) of strain gradient theories deal with the adjustment of special finite element formulations in order to calculate and evaluate second order gradients of displacement [1, 18]. In contrast to them the present study implements a reduced part of the modified strain gradient theory of linear elasticity, *i.e.*, for the case $\ell_0 = \ell_1 = 0$ and $\ell_2 = \ell$. The derivation of the presented variational formulation is consistently based on the balance of linear momentum and on the independent balance of moment of momentum. This procedure provides the possibility of a more or less rational justification of size effects by only referring to the intrinsic rotations.

3.1. A variational formulation for the FE implementation

The starting point is the static balance of linear momentum in its global formulation, without body-forces:

$$0 = \oint_{\partial V} t_j dA = \oint_{\partial V} n_i \sigma_{ij} dA, \tag{11}$$

where t_j represents the force stress vector acting on the surface of the volume V . By applying GAUSS' theorem, the surface integral in Eq. (11) is turned into a volume integral, and the local form of the static balance of linear momentum reads:

$$\int_V \sigma_{ij,i} dV = 0 \Rightarrow \frac{\partial \sigma_{ij}}{\partial x_i} = 0. \tag{12}$$

The global formulation of the static balance of moment of momentum without body-couples is derived analogously [10]:

$$0 = \oint_{\partial V} (\epsilon_{jik} x_i t_k + m_j) dA = \oint_{\partial V} (\epsilon_{jik} x_i n_l \sigma_{lk} + n_i \mu_{ij}) dA . \quad (13)$$

After application of GAUSS' theorem the surface integral in Eq. (13) is turned into a volume integral and the local form of the static balance of moment of momentum becomes [5]:

$$0 = \int_V \left((\epsilon_{jik} x_i \sigma_{lk})_{,l} + \mu_{ij,i} \right) dA = \int_V \left((\epsilon_{jik} x_{i,l} \sigma_{lk} + \epsilon_{jik} x_i \sigma_{lk,l}) + \mu_{ij,i} \right) dA . \quad (14)$$

If symmetry of the force stress tensor $\sigma_{lk} = \sigma_{kl}$ is assumed, and the static balance of linear momentum (Eq. 12) is used, then:

$$\epsilon_{jik} x_{i,l} \sigma_{lk} = \epsilon_{jik} \delta_{il} \sigma_{lk} = \epsilon_{jlk} \sigma_{lk} = 0 , \quad (15)$$

and

$$\epsilon_{jik} x_i \sigma_{lk,l} = 0 , \quad (16)$$

and the local form of the static balance of moment of momentum is:

$$\int_V \mu_{ij,i} dV = 0 \Rightarrow \frac{\partial \mu_{ij}}{\partial x_i} = 0 . \quad (17)$$

The weak formulation of the differential equations (12) and (17) is obtained by multiplication with a variation of the fields of displacement δu_j and rotations $\delta \varphi_j$ (a.k.a. test functions), respectively:

$$\int_V \sigma_{ij,i} \delta u_j dV = 0 \quad \text{and} \quad \int_V \mu_{ij,i} \delta \varphi_j dV = 0 . \quad (18)$$

Due to the arbitrariness and independence of both sets of test functions, the information contained in the original two equations is not affected by the summation:

$$\int_V (\sigma_{ij,i} \delta u_j + \mu_{ij,i} \delta \varphi_j) dV = 0 . \quad (19)$$

By using the rules of integration by parts:

$$\begin{aligned} \int_V \sigma_{ij,i} \delta u_j dV &= \int_V (\sigma_{ij} \delta u_j)_{,i} dV - \int_V \sigma_{ij} \delta u_{j,i} dV , \\ \int_V \mu_{ij,i} \delta \varphi_j dV &= \int_V (\mu_{ij} \delta \varphi_j)_{,i} dV - \int_V \mu_{ij} \delta \varphi_{j,i} dV , \end{aligned} \quad (20)$$

and by applying GAUSS' theorem in its more general formulation including jump terms, the volume integrals in Eq. (20) are turned into surface integrals:

$$\begin{aligned} \int_V (\sigma_{ij} \delta u_j)_{,i} dV &= \oint_{\partial V} \sigma_{ij} \delta u_j n_i dA - \int_S \llbracket \sigma_{ij} \delta u_j \rrbracket n_i dS , \\ \int_V (\mu_{ij} \delta \varphi_j)_{,i} dV &= \oint_{\partial V} \mu_{ij} \delta \varphi_j n_i dA - \int_S \llbracket \mu_{ij} \delta \varphi_j \rrbracket n_i dS . \end{aligned} \quad (21)$$

Since the volume V is decomposed into small subvolumes (discretization) in which the fields of displacement and rotation are approximated polynomially, the continuity of these fields from element to element is not guaranteed yet, and needs to be accounted for by the jump terms. S denotes the singular surfaces that arise from the discretization of the volume. The jump brackets are defined as follows:

$$\begin{aligned} \llbracket \sigma_{ij} \delta u_j \rrbracket n_i &= (\sigma_{ij}^+ \delta u_j^+ - \sigma_{ij}^- \delta u_j^-) n_i , \\ \llbracket \mu_{ij} \delta \varphi_j \rrbracket n_i &= (\mu_{ij}^+ \delta \varphi_j^+ - \mu_{ij}^- \delta \varphi_j^-) n_i , \end{aligned} \quad (22)$$

where $(\cdot)^+$ and $(\cdot)^-$ are the components of a quantity evaluated on the positive side of S minus its evaluation on the negative side. n_i is the surface normal of the corresponding surface, showing into the positive region. By combining Eqs. (19)–(21) we obtain:

$$\begin{aligned} 0 &= - \int_V \sigma_{ij} \delta u_{j,i} dV + \oint_{\partial V} \sigma_{ij} \delta u_j n_i dV - \int_S \llbracket \sigma_{ij} \delta u_j \rrbracket n_i dS \\ &\quad - \int_V \mu_{ij} \delta \varphi_{j,i} dV + \oint_{\partial V} \mu_{ij} \delta \varphi_j n_i dV - \int_S \llbracket \mu_{ij} \delta \varphi_j \rrbracket n_i dS . \end{aligned} \quad (23)$$

By utilizing pre-implemented continuous LAGRANGE finite elements (CG-elements), between which the displacement field is defined as continuous, the jump term given by Eq. (22)₁ is already accounted for and does not need to be incorporated additionally. Furthermore, $\sigma_{ij} n_i$ is replaced by the force stress vector t_j as well as $\mu_{ij} n_i$ is replaced by the couple stress vector m_j , which will be set equal to zero since in practice it is difficult to realize anyway. This leads to:

$$0 = - \int_V (\sigma_{ij} \delta u_{j,i} + \mu_{ij} \delta \varphi_{j,i}) dV + \oint_{\partial V} t_j \delta u_j dV - \int_S \llbracket \mu_{ij} \delta \varphi_j \rrbracket n_i dS . \quad (24)$$

By means of the definitions of the CAUCHY-like force- and couple stress tensors in Eqs. (10)₁ and (10)₄, it can be seen that these measures are symmetric. For this reason and by taking advantage of tensor calculus of symmetric and anti-symmetric tensors, it can be shown that it is equivalent to multiply symmetric tensors by symmetric counterparts. Here, a replacement is performed for $\delta u_{j,i} \Rightarrow \delta \varepsilon_{ij}$ and

$\delta\varphi_{j,i} \Rightarrow \delta\chi_{ij}^S$. Finally, the implemented variational formulation reads:

$$0 = \int_V (\sigma_{ij} \delta\varepsilon_{ij} + \mu_{ij} \delta\chi_{ij}^S) dV - \oint_{\partial V} t_j \delta u_j dV + \int_S \left[\mu_{ij} \delta\varphi_j \right] n_i dS . \quad (25)$$

3.2. Boundary conditions for a cantilever beam

Following a conventional three-dimensional elasto-static finite element analysis of a cantilever beam, the translational and rotational motion of the entire model is suppressed by setting the displacements of the nodes on the clamped surface (at $x = 0$, *cf.*, Fig. 2-a) equal to zero, what is implemented as a DIRICHLET boundary condition. The loading results from defining a constant force stress vector $t_j = (0, 0, -F/A)$ on the surface at $x = L$.

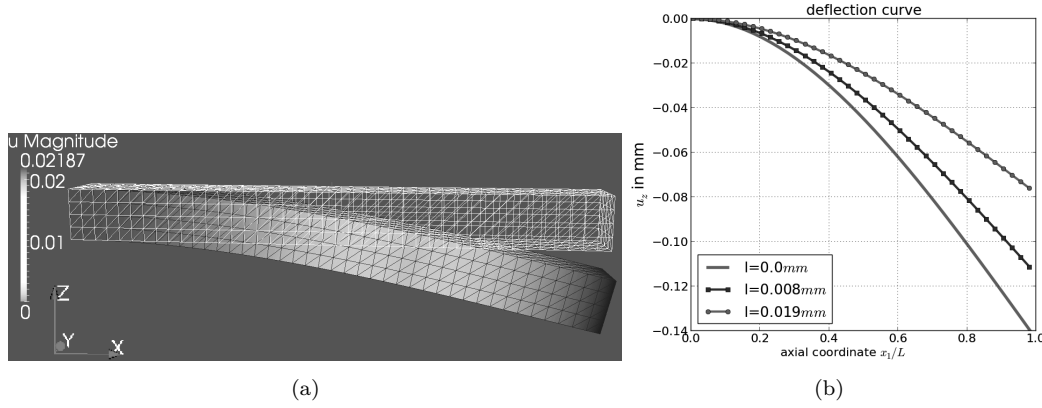


Figure 2. (a) Coordinate system, mesh, and bending mode of the simulation of a cantilever. (b) Numerically evaluated bending line of the model, for different length scale parameters.

In particular, no boundary condition for the microscopic rotation is incorporated due to the direct coupling of the rotation vector to the gradient of displacement. Equation (25) has been implemented in the open-source finite element project FEniCS, which is able to provide a mesh that consists of second order tetrahedra elements in order to account for the second order derivatives of u_i . The GALERKIN method is applied for spatial discretization and the system matrix is solved based on the method of GAUSSIAN elimination. A deviation of less than 5% of deflections in comparison to the CS analytics (*cf.*, Sect. 4) is achieved for a minimum number of elements, if POISSON's ratio is set equal to zero.

4. An analytical approach to Euler-Bernoulli beams

Based on the strain energy density (Eq. 9) for the case $\ell_0 = \ell_1 = 0$ and $\ell_2 = \ell$, the EULER-BERNOULLI assumptions are realized by suitable specification of the form of the displacement vector. The corresponding differential equation:

$$(EI + \mu A \ell^2) w^{IV}(x) = q(x), \quad \forall x \in [0, L] , \quad (26)$$

is then derived by using the principle of virtual work. The bending line in an analytical expression can be obtained by using the following boundary conditions:

$$\begin{aligned} Zw'''(L) &= F, & Zw(0) &= 0, \\ Zw'(0) &= 0, & Zw''(L) &= 0, \end{aligned} \quad (27)$$

where Z is an expression for the bending stiffness, $Z = (EI + \mu A\ell^2)$. The bending line is then given by the following expression:

$$w(x) = -\frac{F}{(EI + \mu A\ell^2)} \left[\frac{x^3}{6} - \frac{Lx^2}{2} \right]. \quad (28)$$

The shear modulus for the analytical approach is $\mu = E/(2 + 2\nu)$, without transformation of E between plain strain and plane stress condition. The bending rigidity is defined to be the ratio of the external force to the deflection of the point where the force is acting. W and T denote the width and the thickness of the beam, respectively. By comparison to the conventional bending rigidity, $D_0 = 3EI/L^3$, and by expanding the second moment of inertia, $I = WT^3/12$, and the area of the cross-section, $A = WT$, the normalized bending rigidity of the present model reads:

$$\frac{D}{D_0} = 1 + \frac{6}{(1 + \nu)} \left(\frac{\ell}{T} \right)^2. \quad (29)$$

This formula depends additionally on the external beam dimension T as well as on the internal length scale parameter ℓ .

5. AFM experiments with epoxy and SU-8

Static bending tests on freestanding beam structures were performed in order to measure the elastic modulus of structures with outer dimensions of a few micrometers. The load F was applied by using the off-axis laser-reflective Atomic Force Microscope (AFM) MultiView-1000 from Nanonics Imaging Ltd.¹ The system consisted of a flat scanner, including a fine thread that is driven by piezo-elements, which need a high-voltage power supply. The detection device works with four Photo-Sensitive Diodes (PSD) interconnected as a WHEATSTONE bridge and monitor deflections of the laser beam path. The laser reflects in an obtuse angle from a fixed AFM-cantilever, such that the system directly monitors its deflections w_c , when it is deformed by the piezo uplift (referred to as the separation z). The raw PSD-signal, obtained in [mV], is converted into forces $F = k_c w_c$ in [μ N] by the help of a calibration procedure. From this procedure the spring constant of the AFM-cantilever was determined as $k_c = 31.4 \text{ N m}^{-1}$. The calibration process is detailed in VARENBERG *et al.* (2005) [17], and was performed by using a precise silicon normal provided by the PTB.² In micro-beam bending tests it can be assumed that the raw AFM-data consists of a

¹www.nanonics.co.il, Jerusalem, Israel

²Physikalisch Technische Bundesanstalt – Braunschweig, Germany

³Fraunhofer Institute for Reliability and Microintegration Berlin, Germany

combined signal of the deflection of the AFM-cantilever and the micro-beam's deflection w in the following manner: $w = z - w_c$. By assuming rectangular cross-sections of the specimens, the following classical relations between the AFM measures F/w , the bending rigidities D and the elastic modulus E are used:

$$D = \frac{F}{w} \quad , \quad D_0 = \frac{3EI}{L^3} \quad , \quad E = \frac{4L^3}{WT^3} \frac{F}{w} . \quad (30)$$

SU-8 is known as the photo-resist NanoTM-SU-8, which is used in micro-system technology (*cf.*, [12]) and produced by the company MicroChem. Structuring of the solid samples (*cf.*, Fig. 3) was carried out in the labs of IZM³. Widths and lengths of the samples were realized in the range of 80–124 μm and 82–920 μm , respectively.



Figure 3. Exemplary SU-8 micro-beam glued to a glass support (on the left hand side) and loaded with a single force by the AFM Tip (on the right hand side). Recorded by optical microscopy.

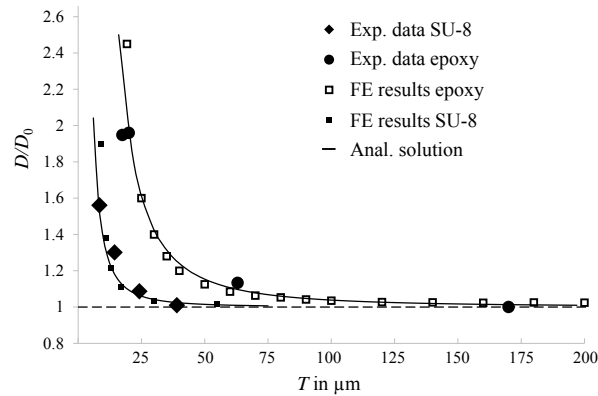


Figure 4. Plot of the results for the experiments on epoxy and SU-8, as well as approximations by analytical solutions and finite element simulations.

The epoxy was processed in the following way: The commercially available resin HT 2 from Poxo Systems was mixed with the appropriate hardener in the ratio 100:48 and put between two preparation glasses within a 45-minute processing time. Different spacers between the preparation glasses assured an adjustable film thickness of 17 – 170 μm . The cured epoxy film was cut into stripes by the help of a parallel cutting tool, which allowed obtaining widths between 100 – 400 μm . The single stripes were glued over the edges of cover glasses. The effective bending length was determined as the distance between the edge of the glass support and the point of force application, and varied between 180 – 4400 μm . The influence of the viscous material behavior of epoxy was investigated by applying different loading rates between 0.1 – 20 $\mu\text{m s}^{-1}$, with only a one percent scatter of the measured values.

6. Results

Based on the experimental work, the material length scale parameter of the modified strain gradient theory can be determined by using a least square method between the experimental data and analytical calculations with the help of the target function of the present theory (Eq. 29).

Table 1. Results

Material	Parameter I	Parameter II
Epoxy	$E = 3.93$ GPa	$\ell = 4.35$ μm
SU-8	$E = 4.14$ GPa	$\ell = 1.39$ μm

When the sizes of structures made of epoxy and SU-8 are reduced, a size effect regarding the bending stiffness occurs. The value of the material length scale parameter for epoxy, which was obtained from measurements in the present work, can now be compared to the literature value [10]. The deviation is about 17%. The variation may be attributed to different manufacturing processes, to a difference in the base materials for the epoxy resin, and to different technical equipment. In summary, bending experiments with differently sized samples can be used to measure the corresponding material length scale parameters of higher-order continuum theories in linear elastostatics. However, attention has to be paid to the fact that an independent quantification of material parameters requires additional modes of deformation. Due to the small scale, difficulties may arise in the experimental techniques. This limitation could serve as an explanation for the sparsity of experimental data for different deformation modes in literature and remains a future challenge.

Acknowledgements

The present work is supported by DFG MU 1752/33-1. The authors wish to thank the Fraunhofer IZM in Berlin for preparation of some of the specimens.

References

- [1] E. Amanatidou, N. Aravas, *Mixed finite element formulations of strain-gradient elasticity problems*, Comput. Methods Appl. Mech. Engrg., **191** (2002), 1723–1751
- [2] A. Bertram, *Finite gradient elasticity and plasticity: a constitutive mechanical framework*, Journal of Continuum Mechanics and Thermodynamics, Springer Berlin Heidelberg (2014), doi: 10.1007/s00161-014-0387-0
- [3] S. Cuenot, C. Fretigny, S. Demoustier-Champagne, B. Nysten, *Surface tension effect on the mechanical properties of nanomaterials measured by atomic force microscopy*, Physical Review B, **69** (2004), 01–05
- [4] F. Dell’Isola, G. Sciarra, S. Vidoli, *Generalized Hooke’s law for isotropic second gradient materials*, Proc. R. Soc. A (2009), doi: 10.1098/rspa.2008.0530
- [5] A.C. Eringen, *Nonlocal continuum field theories*, Springer-Verlag, New York, 2010
- [6] N.A. Fleck, J.W. Hutchinson, *Strain gradient plasticity*, In: Hutchinson J.W., Wu T.Y. (Eds.), Advances in Applied Mechanics, Academic Press, New York, **33** (1997), 295–361
- [7] X.H. Guo, D.N. Fang, X.D. Li, *Measurement of deformation of pure Ni foils by speckle pattern interferometry*, Mechanical in Engineering, **27**, 2 (2005), 21–25
- [8] W.J. Poole, M.F. Ashby, N.A. Fleck, *Micro-hardness of annealed and work-hardened copper polycrystals*, Scripta Materialia, **34**, 4 (1996), 559–564
- [9] W.T. Koiter, *Couple-stresses in the theory of elasticity. Pt. I-II*. Proc. Koninkl. Nederland Akad. Wetensch., **67** (1964), 17–44
- [10] D.C.C. Lam, F. Yang, C.M. Chong, J. Wang, P. Tong, *Experiments and theory in strain gradient elasticity*, J. Mech. Phys. Sol., **51**, 8 (2003), 1477–1508

- [11] Li X.-F., Wang B.-L., Lee K.Y., *Size effect in the mechanical response of nanobeams*. Journal of Advanced Research in Mechanical Engineering, **1**, 1 (2010), 4–16
- [12] H. Lorenz, M. Despon, N. Fahrni, N. LaBianca, P. Renaud, P. Vettiger, *A low-cost negative resist for MEMS*. Journal of Micromechanics and Microengineering, **7** (1997), 121–124
- [13] A.W. McFarland, J.S. Colton, *Role of material microstructure in plate stiffness with relevance to microcantilever sensors*, Journal of Micromechanics and Microengineering, **15**, 5 (2005), 1060–1067
- [14] R.D. Mindlin, H.F. Tiersten, *Effects of couple-stresses in linear elasticity*, ARMA, **11** (1962), 415–448
- [15] R.D. Mindlin, N.N. Eshel, *On first strain-gradient theories in linear elasticity*, International Journal of Solids and Structures, **4** (1968), 109–124
- [16] R.A. Toupin, *Elastic materials with couple-stresses*, ARMA, **11** (1962), 385–414
- [17] M. Varenberg, I. Etsion, G. Halperin, *Nanoscale fretting wear study by scanning probe microscopy*, Tribology Letters, **18**, 4 (2005), 493–498
- [18] Y. Wei, *A new finite element method for strain gradient theories and applications to fracture analyses*, European Journal of Mechanics A/Solids, **25** (2006), 897–913
- [19] F. Yang, C.M. Chong, D.C.C. Lam, P. Tong, *Couple stress based strain gradient theory for elasticity*, International Journal of Solids and Structures, **39**, 10 (2002), 2731–2743